

DEPARTMENT OF STATISTICS
University of Wisconsin
1300 University Ave.
Madison, WI 53706

TECHNICAL REPORT NO. 1121

April 20, 2006

Multi-scale Voxel-based Morphometry via Weighted Spherical Harmonic Representation

Moo K. Chung^{1,2}, Li Shen⁴, Kim M. Dalton²,
Richard J. Davidson^{2,3}

¹Department of Statistics, Biostatistics, and Medical Informatics

²Waisman Laboratory for Brain Imaging and Behavior

³Department of Psychology and Psychiatry

University of Wisconsin-Madison, WI 53706. USA

⁴ Computer and Information Science Department

University of Massachusetts-Dartmouth, MA 02747 USA

`mchung@stat.wisc.edu`

Multi-scale Voxel-based Morphometry via Weighted Spherical Harmonic Representation

Moo K. Chung^{1,2}, Li Shen⁴, Kim M. Dalton², and Richard J. Davidson^{2,3}

¹ Department of Statistics, Biostatistics and Medical Informatics

² Waisman Laboratory for Brain Imaging and Behavior

³ Department of Psychology and Psychiatry

University of Wisconsin-Madison, Madison, WI 53706

⁴ Computer and Information Science Department

University of Massachusetts-Dartmouth, MA 02747

`mchung@stat.wisc.edu`

Abstract. Although the voxel-based morphometry (VBM) has been widely used in quantifying the amount of gray matter of the human brain, the optimal amount of registration that should be used in VBM has not been addressed. In this paper, we present a novel multi-scale VBM using the weighted spherical harmonic (SPHARM) representation to address the issue. The weighted-SPHARM provides the explicit smooth functional representation of true unknown cortical boundary. Based on this new representation, the gray matter tissue density is constructed using the Euclidean distance map from a voxel to the estimated smooth cortical boundary. The methodology is applied in localizing abnormal cortical regions in a group of autistic subjects.

1 Introduction

Voxel-based morphometry (VBM) is a fully automated image analysis technique allowing identification of regional differences in gray matter and white matter between groups of subjects without a prior region of interest in brain magnetic resonance imaging. VBM as implemented in the statistical parametric mapping (SPM) software (<http://www.fil.ion.ucl.ac.uk/spm>) starts with normalizing each structural MRI to the standard SPM template and segmenting it into white and gray matter and cerebrospinal fluid (CSF) based on a Gaussian mixture model [1] [4]. In a slightly different formulation, the tissue density is generated by convolving the binary mask of the tissue with a Gaussian kernel [9]. The resulting density maps are warped into a normalized space and the density are compared across subjects. A modified version of VBM has been also performed along the cortex, where a fraction of gray matter within a ball of radius 15mm is taken as gray matter density [11].

The objective of VBM is to compare regional difference in relative tissue concentration. It is not necessary for image registration used in VBM to match every cortical features exactly, but merely corrects for global brain shape differences. If the image registration was exact, all the segmented images would

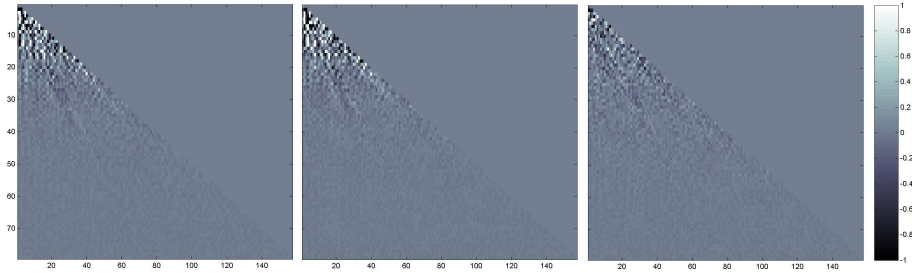


Fig. 1. SPHARM coefficients up to degree $k = 78$ of the outer surface of a subject (vertical direction). The horizontal direction shows the different order within the same degree arranged from $-l$ to l . Left: average of the autistic group. Middle: average of the normal controls. Right: difference between autistic and the normal control groups.

appear identical and no statistically significant differences would be detected [1]. The amount of image registration needed in VBM has been a contentious issue that has yet to be addressed quantitatively [2].

We propose a new methodological framework that enable us to address this issue using the weighted spherical harmonic (SPHARM) representation [?]. The traditional SPHARM is a global parametrization technique that has been applied in anatomical boundaries such as the hippocampus, the amygdala and the brain cortex [6] [7] [10]. The weighed-SPHARM generalizes the traditional SPHARM by weighting each spherical harmonic basis such that the resulting representation becomes the solution of an isotropic diffusion on a unit sphere. The weighted-SPHARM is more suitable than the traditional SPHARM when the realization of the anatomical boundaries, as triangle meshes, are noisy [?]. Since the weighted-SPHARM provides the explicit functional representation of the gray matter boundary, it can be used as a basic descriptive tool for comparing the performance of VBM at different image registration scales.

2 Weighted SPHARM of cortex

Parameterization. Let \mathcal{M}_o and \mathcal{M}_i be the outer (pial) and inner surfaces of the brain respectively. The unit sphere S^2 is realized as a triangle mesh and deformed to match the outer and inner boundaries in such a way that anatomical homology and the topological connectivity of meshes are preserved [8]. The mesh coordinates for the outer surface is then parameterized by the polar angle $\theta \in [0, \pi]$ and the azimuthal angle $\varphi \in [0, 2\pi)$ as $v(\theta, \varphi) = (v_1(\theta, \varphi), v_2(\theta, \varphi), v_3(\theta, \varphi))$. The inner surface is parameterized similarly. These discrete coordinate functions are further parameterized by the SPHARM representation [6] [7] [10]. In SPHARM,

the coordinates are given as

$$v_i(\theta, \varphi) = \sum_{l=0}^k \sum_{m=-l}^l f_{lm}^i Y_{lm}(\theta, \varphi),$$

where Y_{lm} is the spherical harmonics of degree m and order l , and f_{lm}^i is the SPHARM coefficient given by

$$f_{lm}^i = \int_{S^2} v_i(\theta, \varphi) Y_{lm}(\theta, \varphi) \sin \theta d\theta d\varphi.$$

The weighted-SPHARM weights the SPHARM coefficients further such that

$$v_i(\theta, \varphi) = \sum_{l=0}^k \sum_{m=-l}^l e^{-l(l+1)t} f_{lm}^i Y_{lm}(\theta, \varphi). \quad (1)$$

The weighted-SPHARM contains the traditional SPHARM as a special case when $t = 0$. Figure 1 displays the SPHARM coefficients up to degree $k = 78$ with $t = 0.0001$. Anatomical variabilities are encoded in these coefficients. The iterative residual fitting (IRF) algorithm is used for the fast estimation of the SPHARM coefficients [3]. The weighted-SPHARM can be viewed as a smoothing process as stated as the following theorem.

Theorem 1. The equation (1) is the solution of an isotropic diffusion equation

$$\frac{\partial u}{\partial t} = \Delta u \text{ on } S^2, u(\theta, \varphi, t = 0) = v_i(\theta, \varphi),$$

where Δ is the spherical Laplacian.

Stochastic modeling. We model v_i stochastically by assuming f_{lm}^i to follow independent normal distribution $N(\mu_{lm}^i, \sigma_l^2)$ for coordinate i , degree l , and order m . It is natural to assume the equal variability within the same order. This assumption is equivalent to modeling v_i as the sum of signal plus noise:

$$v_i(\theta, \varphi) = \sum_{l=0}^k \sum_{m=-l}^l e^{-l(l+1)t} \mu_{lm}^i Y_{lm}(\theta, \varphi) + \epsilon(\theta, \varphi),$$

where ϵ is a zero mean Gaussian random field with a certain isotropic covariance function. The mean and the variance of the surface is given by

$$\mathbb{E}v_i(\theta, \varphi) = \sum_{l=0}^k \sum_{m=-l}^l e^{-l(l+1)t} \mu_{lm}^i Y_{lm}(\theta, \varphi) \quad (2)$$

$$\mathbb{V}v_i(\theta, \varphi) = \sum_{l=0}^k \sum_{m=-l}^l e^{-2l(l+1)t} \sigma_l^2 Y_{lm}^2(\theta, \varphi)$$

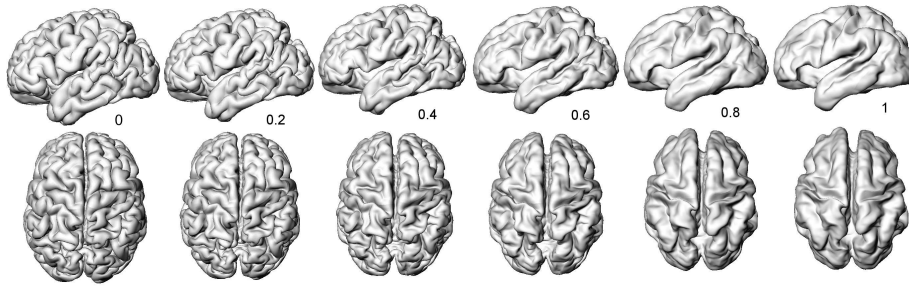


Fig. 2. Multi-scale representation of surface normalization. $\alpha = 0$ shows the surface of one particular subject while $\alpha = 1$ is the average surface of 24 subjects. As α increases, the amount of registration increases toward the average surface.

The total variability of the surface is then measured by

$$\int_{S^2} \mathbb{V}v_i \sin \theta d\theta d\varphi = \sum_{l=0}^k \sum_{m=-l}^l e^{-2l(l+1)t} \sigma_l^2.$$

The optimal degree k is automatically determined by testing the null hypothesis $H_0 : \mu_{lm}^i = 0$ for all $-l \leq m \leq l$ in an iterative fashion for each l . For $t = 0.0001$, the optimal degree is determined to be $k = 78$. Once we determined the optimal degree, we can estimate the unknown parameters μ_{lm}^i and σ_l^2 with the sample mean and the sample variance of the SPHARM coefficients. If

$$v_{ij}(\theta, \varphi) = \sum_{l=0}^k \sum_{m=-l}^l e^{-l(l+1)t} f_{lm}^{ij} Y_{lm}(\theta, \varphi)$$

is the weighted-SPHARM for the j -th subject ($1 \leq j \leq n$), the maximum likelihood estimation of parameters μ_{lm}^i and σ_l^2 is

$$\widehat{\mu}_{lm}^i = \frac{1}{n} \sum_{j=1}^n f_{lm}^{ij}, \quad \widehat{\sigma}_l^2 = \frac{1}{(2l+1)(n-1)} \sum_{m=-l}^l \sum_{j=1}^n (f_{lm}^{ij} - \mu_{lm}^i)^2.$$

The inner surface is modeled similarly.

Surface normalization. In the weighted-SPHARM, the surface normalization is straightforward. Given the weighted-SPHARM representation of two surfaces v_i and w_i , the deformation field d_i that minimizes the integral of the squared errors of registering v_i to w_i is simply given by the following theorem.

Theorem 2. $w_i - v_i = \arg \min_{d_i \in L^2(S^2)} \int_{S^2} (w_i - d_i(v_i))^2 \sin \theta d\theta d\varphi$, The minimization is taken over $L^2(S^2)$, the space of all square integrable functions. Unlike other surface registration algorithms that has been used in registering surfaces, it is not necessary to consider an additional cost function that

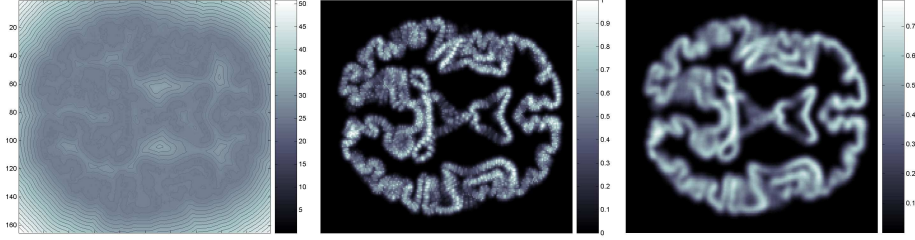


Fig. 3. Left: The contour plot of the average Euclidean distance map from outer and inner surfaces. The color bar is the number of voxels in mm. Middle: gray matter probability map. Right: Gaussian kernel smoothing of the probability map with 10 mm FWHM.

guarantees the smoothness of the deformation field since $w_i - v_i$ is already a linear combination of smooth spherical harmonic basis. Based on this idea, we can register any weighted-SPHARM surface to another weighted-SPHARM surface.

Let \widehat{v}_i be the sample mean surface obtained by replacing μ_{lm}^i with the estimator $\widehat{\mu}_{lm}^i$ in equation (2). This surface can serve as a template for the weighted-SPHARM based surface registration. The displacement from the surface v_{ij} to the template surface is $\Delta v_{ij} = \widehat{v}_i - v_{ij}$. Consider the surface $\mathbf{v}_j(\alpha) = v_{ij} + \alpha \Delta v_{ij} = (1 - \alpha)v_{ij} + \alpha \widehat{v}_i$, which is the trajectory of the deformation from v_{ij} to the template \widehat{v}_i for $0 \leq \alpha \leq 1$ (Figure 2). When $\alpha = 0$, $\mathbf{v}_j(\alpha)$ is surface of the j -th subject while when $\alpha = 1$, it is the template surface. The parameter α controls the amount of registration from the coarse-to-fine scale. The total variability at each scale is computed to be

$$\int_{S^2} \mathbb{V}(\mathbf{v}_j) \sin \theta \, d\theta d\varphi = c(\alpha) \sum_{l=0}^k \sum_{m=-l}^l e^{-2l(l+1)t} \sigma_l^2,$$

where $c(\alpha) = \frac{n-1}{n^2} \alpha^2 + (1 - \frac{n-1}{n} \alpha)^2$ is the decreasing function for $0 \leq \alpha \leq 1$ (Figure 5). The larger the α value, the smaller the image registration variability across the subjects with respect to the template.

Gray matter density. We construct the the gray matter density using the 3D Euclidian distance map of the surfaces at each scale. For the outer surface \mathcal{M}_o , the distance map at each voxel x is defined as $dist_o(x) = \min_{y \in \mathcal{M}_o} \|x - y\|$, where $\|\cdot\|$ is the Euclidian norm. The minimum is found using a nearest neighbor search algorithm on an optimized k-D tree [5]. Similarly we define the distance map for the inner surface \mathcal{M}_i as $dist_i(x) = \min_{y \in \mathcal{M}_i} \|x - y\|$. Then the average distance map is defined as $dist(x) = (dist_o(x) + dist_i(x))/2$. The minimum of $dist$ is always obtained in the middle of the outer and the inner surfaces. Then the gray matter density is defined as

$$p(x) = \exp \left[- \frac{dist_i^2(x) + dist_o^2(x)}{2\rho^2} \right],$$

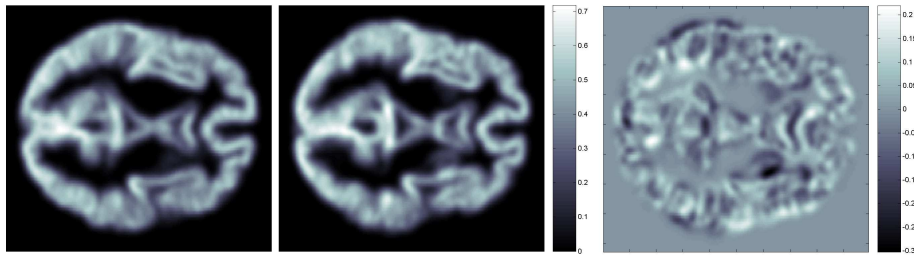


Fig. 4. Mean gray matter density for autism (left) and normal controls (middle) at scale $\alpha = 0$. The right image is the density difference between the two groups. Anatomical variabilities are encoded as the probability of a voxel belonging to the gray matter class.

where parameter ρ^2 controls the spread of density. In this study, we used $\rho^2 = 3$. The gray matter density is always between 0 and 1 and it obtains its maximum in the interior of the gray matter region, where the average distance map obtains the minimum. Then this map is further convoluted with the 3D Gaussian kernel K with 10mm FWHM (full width at the half maximum) to increase the smoothness. The convoluted density map $K * p(x)$ is stochastically modeled as a Gaussian random field. The average distance map is illustrated in Figure 4 for a single subject.

3 Multi-scale voxel-based morphometry

Subjects. We used the constructed gray matter density as an anatomical index for localizing the regions of abnormal amount of gray matter in a group of autistic subjects. $n_1 = 12$ high functioning autistic (HFA) and $n_2 = 12$ normal control (NC) subjects were screened to be right-handed males. Age distributions for HFA and NC are compatible at 15.93 ± 4.71 and 17.08 ± 2.78 respectively. High resolution anatomical magnetic resonance images (MRI) were obtained using a 3-Tesla GE SIGNA scanner with a quadrature head RF coil. A three-dimensional, spoiled gradient-echo (SPGR) pulse sequence was used to generate T_1 -weighted images. Image intensity nonuniformity was corrected using the nonparametric nonuniform intensity normalization method [3] and then the image was spatially normalized into the Montreal neurological institute (MNI) stereotaxic space using a global affine transformation.

Multiscale VBM. Multi-scale representation $\mathbf{v}_i(\alpha)$ at 11 different scales between 0 and 1 with 0.1 increment and its corresponding gray matter density map are constructed. At each scale, we constructed the convoluted density map for each subject. Then the two sample t-test statistic T with the equal variance assumption is computed on the convoluted gray matter density maps. At each voxel x , $T(x)$ is distributed as a student t with $\nu = n_1 + n_2 - 2$ degrees of freedom. Based on the random field theory [12], the corrected p-value is computed using

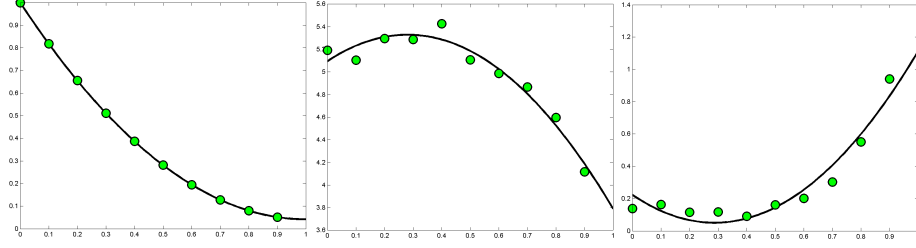


Fig. 5. Left: plot of image registration variability $c(\alpha)$ over scale α . Middle: plot of $\sup T$ statistic value over scale. Right: plot of corrected p-value over scale. At $\alpha = 0.4$, the minimum p-value of 0.0904 is obtained. At other scales the corrected p-value is larger than 0.1. For 90% statistical significance, we may have missed the significant signal at the other scales.

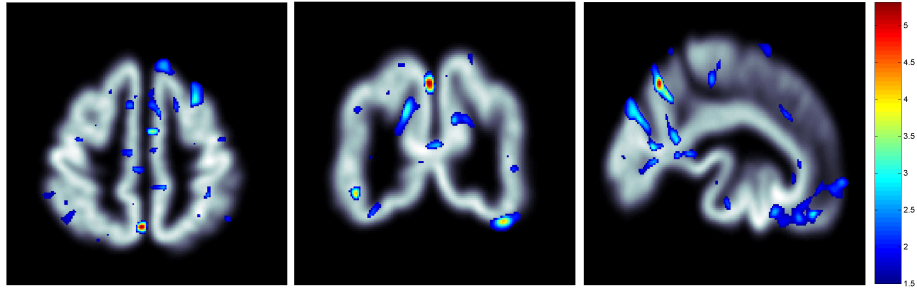


Fig. 6. The final statistical parametric map (t statistics) projected onto the cross sections of the average gray matter density map at scale $\alpha = 0.4$. The positive t statistical values above 1.5 are shown. The cross sections are taken at where the maximum of t statistics occurs.

the following formula:

$$P\left(\sup_{x \in \mathcal{M}_g} T(x) > h\right) \approx \frac{\text{Vol}(\mathcal{M}_g)}{\text{FWHM}^3} \frac{(4 \ln 2)^{3/2}}{(2\pi)^2} \left(\frac{\nu-1}{\nu} h^2 - 1\right) \left(1 + \frac{h^2}{\nu}\right)^{-\frac{\nu-1}{2}},$$

where $\text{Vol}(\mathcal{M}_g)$ is the volume of the gray matter \mathcal{M}_g . The optimal scale is determined to be the one that provides the maximal discrepancy between the groups. Hence, the maximum corrected p value can be chosen as a criteria for determining the optimal scale for VBM. The $\sup_{x \in GM} T(x)$ and its corresponding corrected p-value are plotted in Figure 5 showing the optimal scale is obtained when $\alpha = 0.4$. Figure 6 shows the final statistical parametric map of the optimally chosen VBM.

4 Conclusion

We have presented a new multi-scale VBM that incorporates the convoluted nature of the gray matter using the weighted-SPHARM representation. The explicit mathematical representation of the weighed-SPHARM based surface-to-surface registration enabled us to construct the trajectory of the deformation field. This trajectory is used as a parameter for controlling the amount of image registration in a multi-scale fashion. Then the optimal VBM is chosen that gives the maximal discrimination between the two clinical groups.

References

1. Ashburner, J., Friston, K.J. 2000. Voxel-Based Morphometry - The Methods, *NeuroImage* **11** (2000) 805–821.
2. Bookstein, F.L. Voxel-based morphometry should not be used with imperfectly registered images. *NeuroImage* **14** (2001) 1454–1462.
3. Chung, M.K., Shen, L., Dalton, K.M., Kelley, D.J., Robbins, S.M., Evans, A.C., Davidson, R.J. Weighted spherical harmonic representation and its application to cortical analysis. Technical Report 1118. Dept. of Stat., University of Wisconsin-Madison. <http://www.stat.wisc.edu/~mchung/papers/TR1118.2006.pdf>
4. Davatzikos, C., Genc, A., Xu, D., Resnick, S.M.
Voxel-based morphometry using the RAVENS maps: Methods and validation using simulated longitudinal atrophy. *NeuroImage* **14** (2001) 1361–1369.
5. Friedman, J.H., Bentley, J.L., Finkel, R.A. An algorithm for finding best matches in logarithmic expected Time. *ACM transactions on mathematics software*. **3** (1997) 209–226.
6. Gerig, G., Styner, M., Jones, D., Weinberger, D., Lieberman, J. Shape analysis of brain ventricles using spharm. *MMBIA* (2001) 171–178
7. Gu, X., Wang, Y., Chan, T., Thompson, T., S.T., Y. Genus zero surface conformal mapping and its application to brain surface mapping. *IEEE Transactions on Medical Imaging* **23** (2004) 1–10
8. MacDonald, J., Kabani, N., Avis, D., Evans, A. Automated 3-d extraction of inner and outer surfaces of cerebral cortex from mri. *NeuroImage* **12** (2000) 340–356
9. Paus, T., Zijdenbos, A., Worsley, K., Collins, D.L., Blumenthal, J., Giedd, J.N., Rapoport, J.L., Evans, A.C. Structural maturation of neural pathways in children and adolescents: In Vivo Study. *Science* **283** (1999) 1908–1911.
10. Shen, L., Ford, J., Makedon, F., Saykin, A. surface-based approach for classification of 3d neuroanatomical structures. *Intelligent Data Analysis* **8** (2004)
11. Thompson, P.M., Hayashi K.M., de Zubicaray G., Janke A.L., Rose S.E., Semple J., Herman D., Hong M.S., Dittmer S.S., Doddrell D.M., Toga A.W. Dynamics of gray matter loss in Alzheimer’s disease. *Journal of Neuroscience* **23** (2003) 994–1005.
12. Worsley, K.J., Marrett, S., Neelin, P., Vandal, A.C., Friston, K.J., Evans, A.C. A unified statistical approach for determining significant signals in images of cerebral activation. *Human Brain Mapping* **4** (1996) 58–73.